Since January 2020 Elsevier has created a COVID-19 resource centre with free information in English and Mandarin on the novel coronavirus COVID-19. The COVID-19 resource centre is hosted on Elsevier Connect, the company's public news and information website.

Chaos, Solitons and Fractals 140 (2020) 110166

Contents lists available at ScienceDirect

Chaos, Solitons and Fractals

Nonlinear Science, and Nonequilibrium and Complex Phenomena

journal homepage: www.elsevier.com/locate/chaos

Optimal quarantine strategies for the COVID-19 pandemic in a population with a discrete age structure

João A.M. Gondim [a,*], Larissa Machado [b]

[a] Unidade Acadêmica do Cabo de Santo Agostinho, Universidade Federal Rural de Pernambuco, Cabo de Santo Agostinho, PE, Brazil
[b] Departamento de Matemática, Universidade Federal de Pernambuco, Recife, PE, Brazil

ARTICLE INFO

Article history:
Received 8 June 2020
Revised 20 July 2020
Accepted 26 July 2020
Available online 13 August 2020

Keywords:
COVID-19
Quarantine
SEIR model
Optimal control

ABSTRACT

The goal of this work is to study the optimal controls for the COVID-19 epidemic in Brazil. We consider an age-structured SEIRQ model with quarantine compartment, where the controls are the quarantine entrance parameters. We then compare the optimal controls for different quarantine lengths and distributions of the total control cost by assessing their respective reductions in deaths in comparison to the same period without quarantine. The best strategy provides a calendar of when to relax the isolation measures for each age group. Finally, we analyse how a delay in the beginning of the quarantine affects this calendar by changing the initial conditions.

1. Introduction

At the end of 2019 a novel coronavirus emerged in the city of Wuhan, China. In January 2020 the disease was given the name COVID-19 and, by mid February, China already faced over 60 thousand cases [1]. Many scientists then began to model disease to forecast its worldwide impact [2,3], even influencing policies of many governments.

As the disease spread across Europe and the United States, some countries were forced to implement quarantines or even lockdowns to mitigate the harms and were able to do the so called "flattening of the curve", i.e., to postpone and dampen the maximum number of active cases. By mid May, Brazil is entering this stage, with some states declaring stricter quarantine policies.

Optimal control theory has been applied to general epidemic models [4,5] as well as to specific disease models such as HIV [6–8], tuberculosis [9,10] and influenza [11]. Recently, a few works applying optimal control theory to the COVID-19 pandemic, such as [12] and [13], have appeared. This paper focuses on a SEIR model with quarantine as was proposed in Jia et al. [14], but dividing the population in age groups as in Castilho et al. [15]. This is particularly important since COVID-19 has worse consequences on the elderly than it does on younger people.

Our goal is to calculate the optimal quarantine strategies numerically for different choices of parameters in the model, which reflect the decisions governments must make when implementing these policies, such as evaluating the economical costs of the quarantine for each of the age groups and when to start implementing the measures. Then, we compare the controls by looking at how they reduce deaths in comparison to the same period without quarantine. The best strategy gave us a calendar of when to relax the measures in each of the age groups.

2. The age-structured SEIRQ model

Our model consists of a classical SEIR model with a quarantined class. Besides, we assume that the population has an age structure (see [16,17] for models with a continuous age structure and [18,19] for models with a discrete one). There are three age groups, described in Table 1.

Let $S_i(t)$, $E_i(t)$, $I_i(t)$, $R_i(t)$ and $Q_i(t)$ be the number of susceptible, exposed, infected, recovered and quarantined individuals in each age group at time $t \geq 0$, respectively. We assume that the total population

$$N(t) = \sum_{i=1}^{3} (S_i(t) + E_i(t) + I_i(t) + R_i(t) + Q_i(t))$$

is constant since we are only dealing with a short time frame in comparison to the demographic time scale. The equations, for

* Corresponding author.
E-mail address: joao@dmat.ufpe.br (J.A.M. Gondim).

https://doi.org/10.1016/j.chaos.2020.110166
0960-0779/

Table 1
Description of the age groups.

Age group	Description
1	Young people, aged 0 to 19
2	Adults, aged 20 to 59
3	Elderly, aged 60 onwards.

$i \in \{1, 2, 3\}$, are as follows

$$\begin{aligned} S_i'(t) &= -\frac{S_i(t)}{N(t)}\left(\sum_{j=1}^{3}\beta_{ij}I_j(t)\right) - u_i(t)S_i(t) + \lambda Q_i(t) \\ E_i'(t) &= \frac{S_i(t)}{N(t)}\left(\sum_{j=1}^{3}\beta_{ij}I_j(t)\right) - \sigma_i E_i(t) \\ I_i'(t) &= \sigma_i E_i(t) - \gamma_i I_i(t) \\ R_i'(t) &= \gamma_i I_i(t) \\ Q_i'(t) &= u_i(t)S_i(t) - \lambda Q_i(t). \end{aligned} \tag{1}$$

All parameters are nonnegative. β_{ij} is the transmission coefficient from age group i to age group j. Typically, it will be assumed that $\beta_{ij} = \beta_{ji}$ for all i, j. σ_i and γ_i are the latency and recovery periods, respectively, for age group i. λ is the exit rate from the quarantine. Our controls are the $u_i(t)$, which denote the fraction of susceptible individuals in each age group that are put into quarantine per unit time at t. As such, they satisfy, a priori,

$$0 \le u_i(t) \le 1 \quad i \in \{1, 2, 3\}. \tag{2}$$

However, it is unrealistic to expect an entire population to stay under quarantine for a long time. There are essential workers such as healthcare professionals and police officers that cannot stay at home during these times. As most of these workers are in age group 2, we suppose that all of age groups 1 and 3 can be quarantined (for age group 3, indeed, this is especially important since they are a risk group for the COVID-19 pandemic). Thus, we shall loosen (2) by considering, for example,

$$0 \le u_2(t) \le u_{\max}.$$

Evaluating $u_{\max}$ is one of the tasks of each government's authorities. In this paper, we fix this parameter at $u_{\max} = 0.9$. This means that

$$0 \le u_1(t) \le 1, \quad 0 \le u_2(t) \le 0.9, \quad 0 \le u_3(t) \le 1. \tag{3}$$

Let

$$N_i(t) = S_i(t) + E_i(t) + I_i(t) + R_i(t) + Q_i(t)$$

be the total population of age group i. Adding the equations in the system above, we see that $N_i(t)$ is also constant for $i \in \{1, 2, 3\}$. Since $R_i(t)$ only appears in the other equations as a part of $N_i(t)$, we substitute the equations for $R_i'i(t)$ by $N_i'(t)$. Hence, we may also consider the system of

$$\begin{aligned} S_i'(t) &= -\frac{S_i(t)}{N(t)}\left(\sum_{j=1}^{3}\beta_{ij}I_j(t)\right) - u_i(t)S_i(t) + \lambda Q_i(t) \\ E_i'(t) &= \frac{S_i(t)}{N(t)}\left(\sum_{j=1}^{3}\beta_{ij}I_j(t)\right) - \sigma_i E_i(t) \\ I_i'(t) &= \sigma_i E_i(t) - \gamma_i I_i(t) \\ Q_i'(t) &= u_i(t)S_i(t) - \lambda Q_i(t) \\ N_i'(t) &= 0. \end{aligned} \tag{4}$$

Parameter values are taken from [15] and are listed in Table 2. The data fitting was performed using an adaptation of a least-squares algorithm from [20].

Table 2
Parameter values (data from [15]).

Parameter	Value	Parameter	Value
β_{11}	1.76168	σ_1	0.27300
β_{12}	0.36475	σ_2	0.58232
β_{13}	1.32468	σ_3	0.69339
β_{22}	0.63802	γ_1	0.06862
β_{23}	0.35958	γ_2	0.03317
β_{33}	0.57347	γ_3	0.35577

Table 3
Number of cases, deaths and recoveries by age group [21].

Age group	Cases	Deaths	Recoveries
1	2448	7	2441
2	113,059	891	112,168
3	121,928	17,948	103,980
Total	237,435	18,846	218,589

Table 4
Distribution of infections and recoveries by age group.

Age group	% of cases	% of recoveries
1	1.03%	1.12%
2	47.62%	51.31%
3	51.35%	47.57%
Total	100%	100%

To see how the numbers of infections and recoveries are distributed in the three age groups, we refer to the data available in Centro [21], shown in Table 3. For simplification, we suppose that the difference between the number of cases and the number of deaths represents the number of recoveries. This is not necessarily correct, because some of the patients that we considered as recovered might still carry the disease, but we use this approach due to the scarcity of information regarding recoveries we currently have. The respective distributions are shown in Table 4.

According to [1], Brazil had as of May 13, 2020 a total of 97,575 active COVID-19 cases. Even though there seems to be a large underreporting in the country [22], this number will be considered as the total number of infected individuals nonetheless. To estimate the number of exposed cases, we look at data from May 8, 2020, since the mean incubation period of the disease is thought to be around 5 days [23]. Once again according to [1], at this time Brazil had 76,603 active cases, so this gives us an estimation of 20,972 exposed cases. We also suppose that these cases follow the age distributions of cases from Table 4. Finally, as of May 8, there were 65,124 recovered cases in Brazil [1].

Therefore, our initial time will consist of data from Brazil as of May 8, 2020. The total population is assumed to be 200 million, divided into 40% young people, 50% adults and 10% elderly. We also assume that there are no quarantined individuals when the simulation starts. Since the numbers of exposed, infected and recovered are very small in comparison to the total population, we assume that the initial number of susceptible individuals is equal to the total population of the respective age group. The initial conditions of all variables, rounded to the nearest integers, are listed in Table 5.

3. The optimization problem

Using system (4), we consider the functional to be minimized as

$$J = \int_0^T \sum_{i=1}^{3}\left(I_i(t) + B_i u_i^2(t)\right)dt \tag{5}$$

Table 5
Initial conditions.

Class	$i = 1$	$i = 2$	$i = 3$
Susceptible	80 million	100 million	20 million
Exposed	216	9987	10,769
Infected	789	36,478	39,335
Recovered	729	33,415	30,979
Quarantined	0	0	0

In the formula above, T is the quarantine duration and the parameters B_i are the costs of the control. We assume that $B_i > 0$ for $i \in \{1, 2, 3\}$ and that

$$B_1 + B_2 + B_3 = B, \tag{6}$$

where $B \in \mathbb{R}$ is the total control cost. Sufficient conditions for the existence of the optimal controls follow from standard results from optimal control theory. For instance, we can use Theorem 2.1 in Joshi et al. [24] to show that the optimal control exists. Pontryagin's maximum principle [25,26] establish that optimal controls are solutions of the Hamiltonian system with Hamiltonian function

$$\begin{aligned} H = &\sum_{i=1}^{3} \left(I_i(t) + B_i u_i^2(t)\right) \\ &+ \sum_{i=1}^{3} \left(\lambda_i^S S_i'(t) + \lambda_i^E E_i'(t) + \lambda_i^I I_i'(t) + \lambda_i^Q Q_i'(t) + \lambda_i^N N_i'(t)\right), \end{aligned} \tag{7}$$

where λ_i^S, λ_i^E, λ_i^I, λ_i^Q and λ_i^N are the adjoint variables. These variables must satisfy the adjoint equations

$$\lambda_i^{C\prime} = -\frac{\partial H}{\partial C_i}, \tag{8}$$

where $i \in \{1, 2, 3\}$ and $C \in \{S, E, I, Q, N\}$. The adjoint system is detailed in (9) below.

$$\begin{aligned} \lambda_i^{S\prime} &= \frac{1}{N}\left(\sum_{j=1}^{3} \beta_{ij} I_j\right)\left(\lambda_i^S - \lambda_i^E\right) + u_i(t)\left(\lambda_i^S - \lambda_i^Q\right) \\ \lambda_i^{E\prime} &= \sigma_i\left(\lambda_i^E - \lambda_i^I\right) \\ \lambda_i^{I\prime} &= -1 + \frac{1}{N}\sum_{j=1}^{3} \beta_{ji} S_j\left(\lambda_j^S - \lambda_j^E\right) + \gamma_i \lambda_i^I \\ \lambda_i^{Q\prime} &= \lambda\left(\lambda_i^Q - \lambda_i^S\right) \\ \lambda_i^{N\prime} &= \frac{1}{N^2}\sum_{k=1}^{3}\sum_{j=1}^{3} \beta_{kj} S_k I_j\left(\lambda_k^E - \lambda_k^S\right). \end{aligned} \tag{9}$$

The adjoint variables also must satisfy the transversality conditions

$$\lambda_I^S(T) = \lambda_i^E(T) = \lambda_i^I(T) = \lambda_i^Q(T) = \lambda_i^N(T) = 0, \tag{10}$$

for $i \in \{1, 2, 3\}$.

Finally, the optimality conditions come from solving

$$\frac{\partial H}{\partial u_i} = 0. \tag{11}$$

This results in

$$u_i^* = \frac{\left(\lambda_i^S - \lambda_i^Q\right) S_i}{2B_i}. \tag{12}$$

Since we are considering bounded controls (because of (3)), the u_i^* are calculated using

$$u_i^* = \min\left\{u_{\max}^i, \max\left\{0, \frac{\left(\lambda_i^S - \lambda_i^Q\right) S_i}{2B_i}\right\}\right\}, \tag{13}$$

where $u_{\max}^1 = u_{\max}^3 = 1$ and $u_{\max}^2 = 0.9$.

Uniqueness of the optimal controls (at least for small enough T) also follow from standard results, such as Theorem 2.3 in Joshi et al. [24]. Numerical solutions of systems (4) and (9) can be found by a forward-backward sweep method [26]. The algorithm starts with an initial guess of the controls u_1, u_2 and u_3 and then solves (4) forward in time. After this first part, it uses the results and the initial guesses to solve (9) backward in time and new controls are defined following (13). This process continues until it converges.

4. Comparison of optimal controls for different control costs

Quarantines are not just a matter of public health, for they also present economic questions, for example. This means that we must pay close attention to the control costs B_i. These numbers reflect how the population is capable of dealing with the quarantine of the respective age group. Smaller values of B_i mean that the population can withstand a stricter quarantine without many economical side effects. This is not possible, on the other hand, for bigger values of B_i.

Since the bigger economic toll of the quarantine lies on the adults (because they form almost all of the economically active population), we assume that B_2 is the greatest of the three values. As the isolation of the young implies closing schools, this educational impact makes B_1 the second highest cost, albeit much smaller than B_2.

How the total cost B is distributed among the age groups determines the shape of the optimal controls. To study this relation, we let $B = 5000$, with $B_2 \in [3600, 4600]$ and $B_3 \in [10, 110]$. For our simulations, we consider $B_2 \in \{3600 + 50k : 0 \le k \le 20\}$ and $B_3 \in \{10 + 5k : 0 \le k \le 20\}$. This means that 441 cost distributions will be analysed for each quarantine length.

Our goal now is to compare these distributions by investigating the number of deaths caused by the pandemic at the end of the quarantine for each one of them. As in Castilho et al. [15], the deaths will be calculated as a fraction of the recovered, since there is no disease induced mortality in our model. From Table 3, we can derive the case fatality rates μ_1, μ_2 and μ_3 for age groups 1, 2 and 3, respectively. The results are

$$\begin{aligned} &\mu_1 = \frac{7}{2448} = 0.003, \quad \mu_2 = \frac{891}{113,059} = 0.008, \\ &\mu_3 = \frac{17,948}{121,928} = 0.147. \end{aligned} \tag{14}$$

Let $\mathcal{D}(b_2, b_3, t)$ and $R_i(b_2, b_3, t)$, $i \in \{1, 2, 3\}$, denote the cumulative number of deaths due to the disease at time t and the number of recovered individuals in the optimal control problem for age group i, respectively, for the cost distribution with $B_2 = b_2$ and $B_3 = b_3$. By our discussion above, we can write

$$\mathcal{D}(b_2, b_3, t) = \mu_1 R_1(b_2, b_3, t) + \mu_2 R_2(b_2, b_3, t) + \mu_3 R_3(b_2, b_3, t). \tag{15}$$

Fig. 1 shows plots of $\mathcal{D}(B_2, B_3, T)$ as a function of B_2 and B_3. Because of the uncertain nature of the parameters and due to the high number of unreported cases, we do not show the crude numbers of $\mathcal{D}(B_2, B_3, T)$ for the 441 distributions. The approach we use instead is to select the smallest values for each quarantine length as unit and then scale the other values accordingly.

According to [22], ratio estimates of reported to unreported cases vary from 1:1 to 1:20. This ratio introduces a multiplicative factor in the numbers of exposed, infected and recovered individuals which is cancelled since we are dealing with relative proportions.

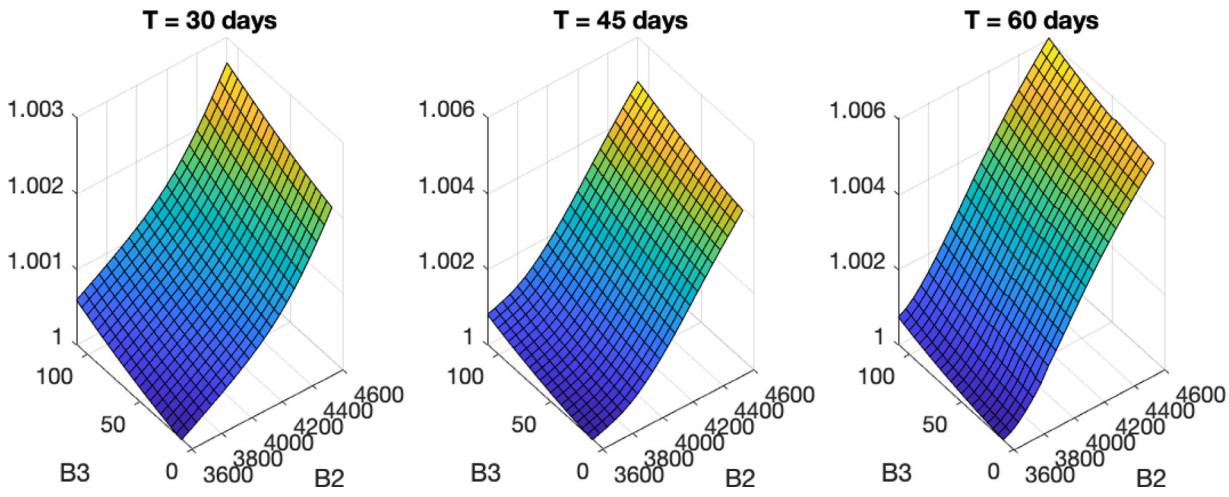

Fig. 1. Plots of the scaled $\mathcal{D}(B_2, B_3, T)$ as a function of B_2 and B_3 for quarantine lengths of 30, 45 and 60 days.

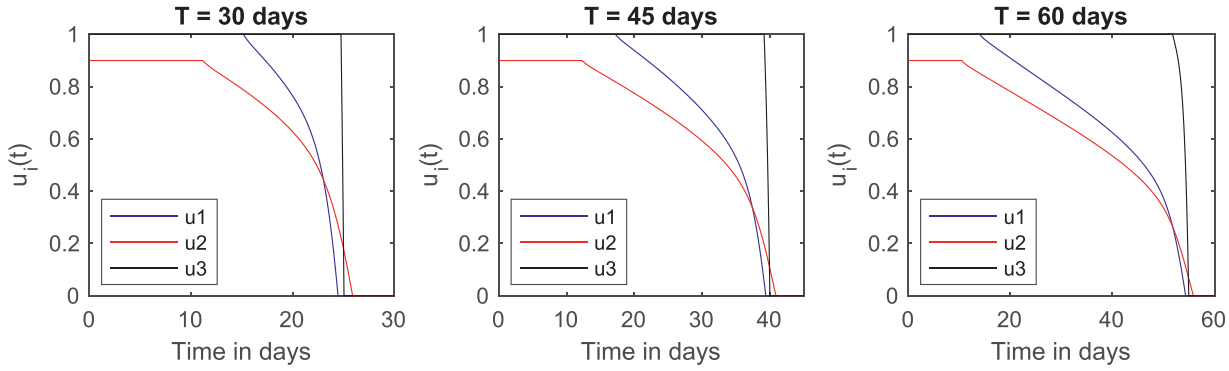

Fig. 2. Plots of $\mathcal{D}(t)/\mathcal{D}(3600, 10, T)$ for different quarantine lengths.

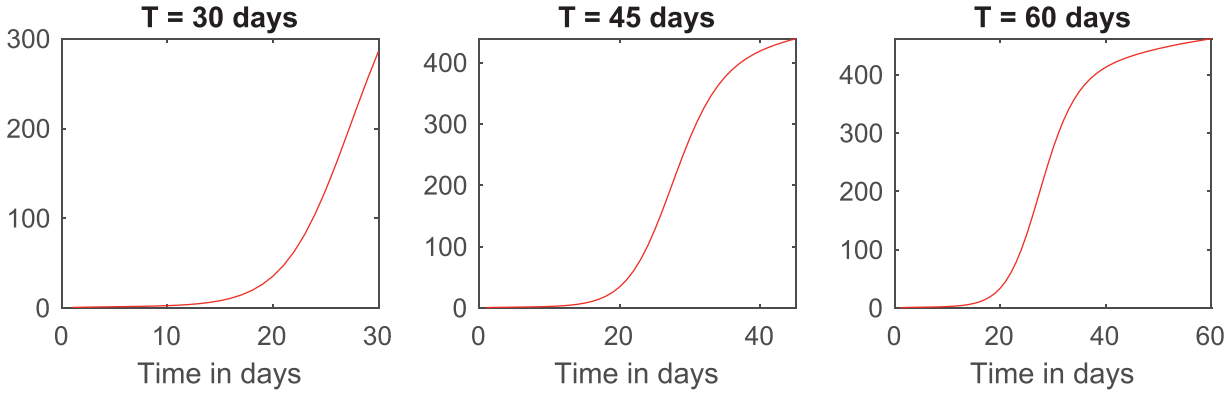

Fig. 3. The optimal controls for $B_1 = 1390$, $B_2 = 3600$ and $B_3 = 10$ for different quarantine lengths.

Notice that, in all three cases, the distribution with the lowest number of deaths is $B_1 = 1390$, $B_2 = 3600$ and $B_3 = 10$. To assess how the optimal quarantines reduce deaths for this cost distribution, we let $\mathcal{D}(t)$ be the cumulative number of deaths for the model with no quarantine. In Fig. 2, we plot graphs of $\mathcal{D}(t)$ divided by $\mathcal{D}(3600, 10, T)$ for $T = 30$, 45 and 60 days. At the end of the quarantine, the optimal controls reduce the number of deaths in 286, 439 and 461 times, respectively.

Fig. 3 plots the graphs of the optimal controls $u_1(t)$, $u_2(t)$ and $u_3(t)$ for this cost distribution. An interesting feature of these plots is that they provide an "optimal calendar" of when the quarantine should start to be relaxed. This calendar is shown in Table 6.

Table 6
How long it takes until quarantine relaxation.

Age group	$T = 30$	$T = 45$	$T = 60$
1	16 days	18 days	14 days
2	12 days	13 days	11 days
3	25 days	39 days	52 days

We acknowledge that the elderly are not the only risk group for the Covid-19 epidemic, since people with comorbidities such as obesity, diabetes and hypertension also present higher case fatality rates, even though these factors were not considered in our

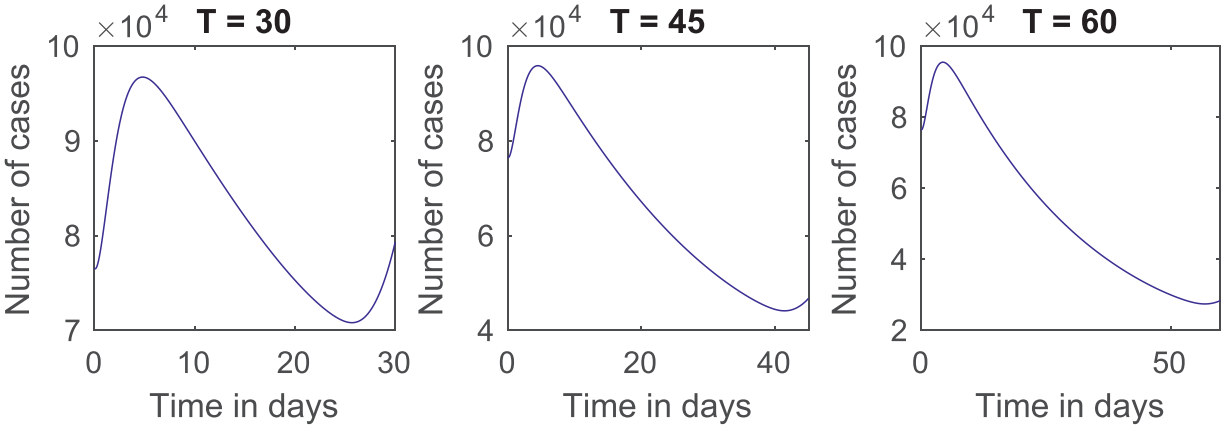

Fig. 4. Curves of infections for quarantines of 30, 45 and 60 days and cost distribution $B_1 = 1390$, $B_2 = 3600$, $B_3 = 10$.

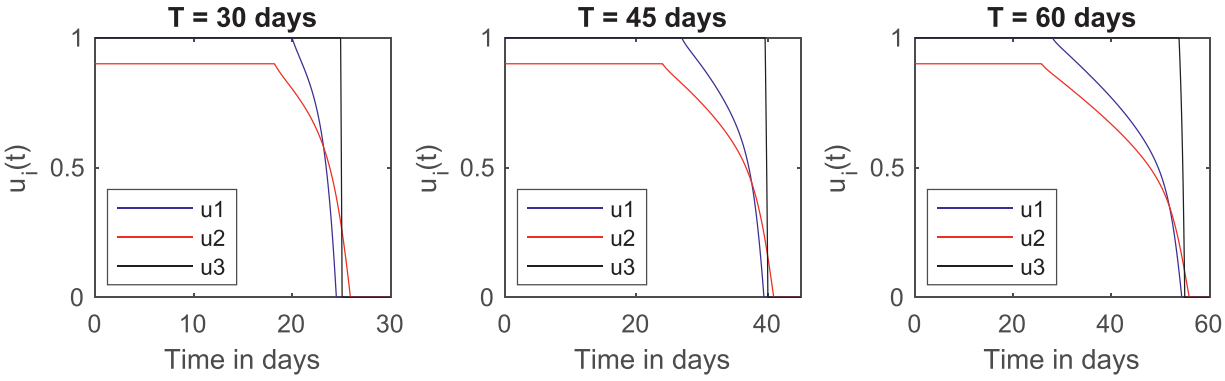

Fig. 5. Plots of the optimal controls for different quarantine lengths. Initial conditions of exposed, infected and recovered are doubled.

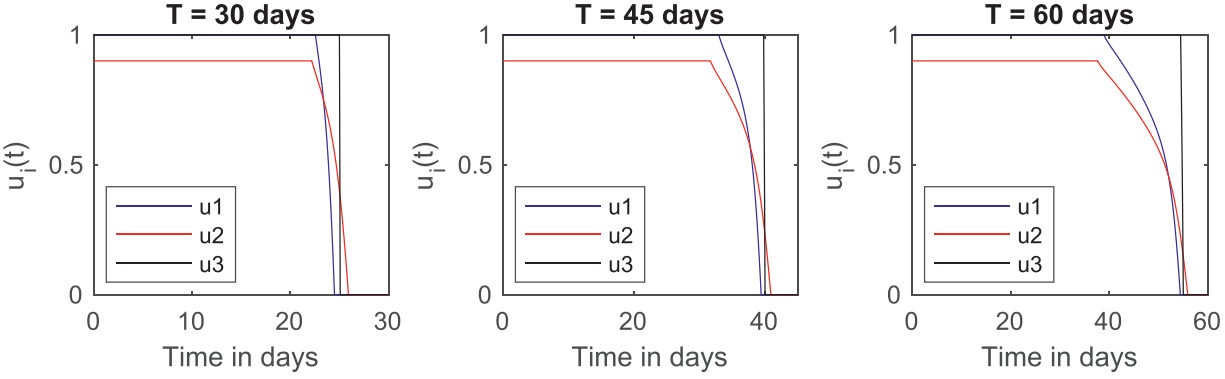

Fig. 6. Plots of the optimal controls for different quarantine lengths. Initial conditions of exposed, infected and recovered are multiplied by four.

model. Thus, we emphasize that the quarantines for these individuals should also follow the relaxation calendar of the elderly, independently of their age group.

We now investigate how the length of the quarantine influences its effectiveness by plotting the total number of infections for the cost distribution $B_1 = 1390$, $B_2 = 3600$ and $B_3 = 10$ in Fig. 4.

The three curves reach their minimum around the same time that the controls reach zero. For quarantines of 45 and 60 days, the number of cases at the end is, indeed, much smaller than it is in the beginning. However, for the shorter quarantine, there are more cases in the end than the initial total.

This fact shows that quarantines cannot be too short, or else the overall situation in the end could be worse than in the beginning. Moreover, the number of cases starts to go up again towards the end in all three cases.

To finish this Section, we analyse how the initial conditions affect the optimal control. We can interpret this as a way to see what happens if it takes too long for these measures to be implemented. We do this by considering initial conditions of exposed, infected and recovered twice and four times as much as their original values. As of May 13, 2020, the number of active cases in Brazil doubles every 10 days [1], so this means waiting 10 or 20 days, respectively, to start the quarantine. In the plots of Figs. 5 and 6, we consider distribution $B_1 = 1390$, $B_2 = 3600$ and $B_3 = 10$ with initial conditions twice and four times their original values, respectively. They provide different relaxation calendars, which are described in Tables 7 and 8.

A comparison of Tables 6–8 shows that the quarantines have to be much stricter if there is a delay in their implementation. Moreover, as we did in Fig. 2, we look at the reduction in

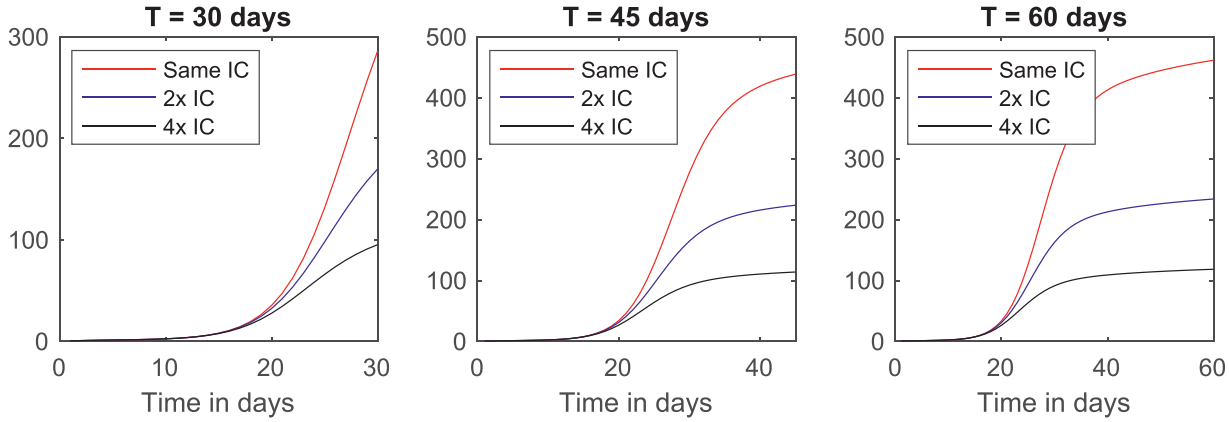

Fig. 7. Plots of $\mathcal{D}(t)/\mathcal{D}(3600, 10, T)$ for different quarantine lengths and initial conditions of exposed, infected and recovered.

Table 7
Times until relaxation for $B_1 = 1390$, $B_2 = 3600$ and $B_3 = 10$. Initial conditions of exposed, infected and recovered are doubled.

Age group	$T = 30$	$T = 45$	$T = 60$
1	20 days	27 days	28 days
2	19 days	24 days	26 days
3	25 days	40 days	54 days

Table 8
Times until relaxation for $B_1 = 1390$, $B_2 = 3600$ and $B_3 = 10$. Initial conditions of exposed, infected and recovered are multiplied by four.

Age group	$T = 30$	$T = 45$	$T = 60$
1	23 days	33 days	39 days
2	23 days	32 days	38 days
3	25 days	40 days	55 days

deaths at the end of the quarantine in Fig. 7. The plots show that:

1. For quarantines of 30 days, the optimal controls reduce the number of deaths in 170 and 95 times for initial conditions of exposed, infected and recovered twice and four times their original values, respectively, instead of reducing it in 286 times as before.
2. For quarantines of 45 days, the reduction in the number of deaths is in 224 and 114 times for initial conditions twice and four times their original values, respectively, instead of 439 times.
3. For quarantines of 60 days, the reduction is in 234 and 119 times for initial conditions twice and four times the original values, respectively, instead of 462 times.

Hence, the longer it takes for the quarantine to start, the less effective it is.

5. Conclusions

In this paper we considered an age-structured SEIRQ model, where the quarantine entrance parameters are thought as controls of the system, and we looked for the optimal controls via Pontryagin's maximum principle. After writing down the optimality system, we calculated the optimal controls numerically and analysed how some of the parameters influence the results.

These parameters represent the difficult choices authorities must make, such as deciding how many essential workers are allowed to remain circulating, estimating the economic impact of the quarantine and even when to start it. As such choices are made, the optimal controls give guidelines of how to proceed.

In Section 4, we considered a constant total control cost and distributed it among the age groups in 441 ways. The distribution with the best results with regard to deaths during the quarantine gave us a calendar of when to relax the isolation measures in the three age groups (for quarantine lengths of 30, 45 and 60 days, respectively):

- For the youngs, the date of relaxation was the 16th, the 18th or the 14th day.
- For the adults, the relaxation started at the 12th, the 13th or the 11th day.
- For the elderly, it started at the 25th, the 39th or the 52nd day.

The optimal controls that induce this calendar produced a reduction in the number of deaths of 286, 439 and 462 times, respectively, in comparison to the same period of time without quarantine. However, in the three cases the number of infected cases reached a minimum just before the end of the simulation, so by the time the quarantine ended, the cases were going up again, even becoming bigger than the original values for the shorter length we considered. This shows that the quarantines are not effective if they are not long enough.

We also showed that waiting too long to start the quarantine makes the period before the relaxation become longer. This also produced a loss in efficacy, since the reduction of deaths due to the quarantine (in comparison to the "doing nothing" scenario) decreased as the number of initial cases increased.

In our model we used data from Brazil as initial conditions and in the parameter fitting. Brazil is a very large country, with many cities at different stages of the pandemic. This means that studies such as this one should be made locally to best suit the characteristics of each city. As the plots of Figs. 5 and 6 suggest, the sooner the quarantine is implemented, the shortest the time the controls need to stay at their maximum is.

Finally, we acknowledge that not all individuals have the same possibility of fulfilling the quarantine. In countries with severe socioeconomic inequalities such as Brazil, the wealthier citizens have much more resources to go through the isolation period than the poorer [27]. We did not include these factors in our model. However, many countries around the world have provided financial support for those in need [28] in an attempt to mitigate this problem during the pandemic.

Declaration of Competing Interest

The authors declare that they have no known competing financial interests or personal relationships that could have appeared to influence the work reported in this paper.

CRediT authorship contribution statement

João A.M. Gondim: Conceptualization, Methodology, Software, Formal analysis, Investigation, Data curation, Writing - original draft, Writing - review & editing, Supervision. **Larissa Machado:** Software, Validation, Resources, Writing - review & editing.

Acknowledgement

The authors would like to thank César Castilho (UFPE) for all the valuable discussions and suggestions during the preparation of this manuscript.

References

[1] Worldometers. https://www.worldometers.info/coronavirus/; Accessed: 2020-05-15.
[2] Wu JT, Leung K, Leung GM. Nowcasting and forecasting the potential domestic and international spread of the 2019-nCoV outbreak originating in wuhan, china: a modelling study. Lancet 2020;395(10225):689–97.
[3] Ferguson N., Laydon D., Nedjati Gilani G., Imai N., Ainslie K., Baguelin M., et al. Report 9: impact of non-pharmaceutical interventions (NPIS) to reduce COVID19 mortality and healthcare demand 2020.
[4] Behncke H. Optimal control of deterministic epidemics. Optim Control Appl Methods 2000;21(6):269–85.
[5] Mateus JP, Rebelo P, Rosa S, Silva CM, Torres DF. Optimal control of non-autonomous SEIRS models with vaccination and treatment. Discrete Cont Dyn S 2018;11(6):1179–99.
[6] Joshi HR. Optimal control of an HIV immunology model. Optim Control Appl Methods 2002;23(4):199–213.
[7] Fister KR, Lenhart S, McNally JS. Optimizing chemotherapy in an HIV model. Electron J Differ Equ 1998;1998(32):1–12.
[8] Kirschner D, Lenhart S, Serbin S. Optimal control of the chemotherapy of HIV. J Math Biol 1997;35(7):775–92.
[9] Silva CJ, Torres DF. Optimal control for a tuberculosis model with reinfection and post-exposure interventions. Math Biosci 2013;244(2):154–64.
[10] Jung E, Lenhart S, Feng Z. Optimal control of treatments in a two-strain tuberculosis model. Discrete Contin Dyn Syst B 2002;2(4):473.
[11] Lee S, Chowell G, Castillo-Chávez C. Optimal control for pandemic influenza: the role of limited antiviral treatment and isolation. J Theor Biol 2010;265(2):136–50.
[12] Grigorieva E., Khailov E., Korobeinikov A.. Optimal quarantine strategies for COVID-19 control models. arXiv preprint arXiv:200410614 2020.
[13] Djidjou-Demassea R., Michalakisa Y., Choisya M., Sofoneaa M., Alizona S.. Optimal COVID-19 epidemic control until vaccine deployment. medrxiv. https://doi.org/10.1101/2020.04.02.20049189.
[14] Jia J, Ding J, Liu S, Liao G, Li J, Duan B, et al. Modeling the control of COVID-19: impact of policy interventions and meteorological factors. Electron J Differ Equ 2020;2020(23):1–24.
[15] Castilho C, Gondim JAM, Marchesin M, Sabeti M. Assessing the efficiency of different control strategies for the COVID-19 epidemic. Electron J Differ Equ 2020;2020(64):1–17.
[16] Thieme H. Disease extinction and disease persistence in age structured epidemic models. Nonlinear Anal Theory Methods Appl 2001;47(9):6181–94.
[17] Inaba H. Mathematical analysis of an age-structured sir epidemic model with vertical transmission. Discrete Contin Dyn Syst B 2006;6(1):69.
[18] Zhou Y, Fergola P. Dynamics of a discrete age-structured sis models. Discrete Contin Dyn Syst B 2004;4(3):841.
[19] Zhou L, Wang Y, Xiao Y, Li MY. Global dynamics of a discrete age-structured sir epidemic model with applications to measles vaccination strategies. Math Biosci 2019;308:27–37.
[20] Martcheva M. An introduction to mathematical epidemiology, 61. Springer; 2015.
[21] Centro de coordinación de alertas y emergencias sanitarias goberno españa - enfermedad por el coronavirus (COVID-19). https://www.mscbs.gob.es/profesionales/saludPublica/ccayes/alertasActual/nCov-China/documentos/Actualizacion_104_COVID-19.pdf. Accessed: 2020-05-15; 2020.
[22] Russel T.. Using a delay adjusted case fatality ratio to estimate under reporting; 2020. https://cmmid.github.io/topics/covid19/global_cfr_estimates.html.
[23] Lauer SA, Grantz KH, Bi Q, Jones FK, Zheng Q, Meredith HR, et al. The incubation period of coronavirus disease 2019 (COVID-19) from publicly reported confirmed cases: estimation and application. Ann Intern Med 2020;172(9):577–82.
[24] Joshi HR, Lenhart S, Li MY, Wang L. Optimal control methods applied to disease models. Contemp Math 2006;410:187–208.
[25] Pontryagin LS. Mathematical theory of optimal processes. Routledge; 2018.
[26] Lenhart S, Workman JT. Optimal control applied to biological models. CRC Press; 2007.
[27] Lockdowns are fine for the rich, but millions are too poor to shelter from coronavirus. https://tinyurl.com/nbcnews-lockdowns; Accessed: 2020-07-20.
[28] Coronavirus bailouts: Which country has the most generous deal? https://www.bbc.com/news/business-52450958; Accessed: 2020-07-18.